TECHNICAL PAPER

Influence of CNT volume fractions on static and dynamic behavior of aluminum honeycomb-cored carbon-fiber-reinforced honeycomb sandwich structure

Shubham Chandra[1] · Amit Amulani[1] · Shweta B. Thomas[2] · Sourabh Kumar Soni[3] · Benedict Thomas[1]

Abstract

Sandwich structures made up of honeycomb composites have high-strength structural applications because of their low weight and high stiffness. High flexural stiffness is a major aspect in developing structures with several multilayer materials. Statistical tests analyze the behavior of loads to which a body can sustain without failure and dynamic behavior defines the overall failure modes and the vibration characteristics. In this study, static and dynamic responses of honeycomb sandwich structures are performed under static load conditions. The structures made up of carbon fiber reinforcement including various volume fractions of carbon nanotubes (CNT) used as face sheets and aluminum 3003 as core were prepared. Four distinct combinations were examined in this investigation, including one where the face sheet was made primarily of carbon fiber and epoxy without CNT and three others where CNT was added into the matrix with 2 w%, 5 w% and 7.5 w%, respectively. The three-point bending test was performed according to the ASTM standard C393 experimentally and the validation was performed computationally using ANSYS. Free vibration test was carried out analyzing different mode shapes and natural frequencies. In static tests, there was a high correlation between experimental and simulation results. The obtained results reveal the exceptional behavior of the proposed honeycomb structure. The proposed material combination is anticipated to show a high degree of pragmatism in aeronautical applications based on the findings.

1 Introduction

Composite structures are formulated with two or more different materials that contain reasonable properties and form a single component used in various applications. The benefit of adopting composite materials is their high rigidity, strength and their longer fatigue life which allows for weight reduction in the design. They provide further resistance to corrosion, fatigue strength, durability, thermal stability

✉ Benedict Thomas
benedict.thomas@vit.ac.in

1 School of Mechanical Engineering, VIT, Vellore, Tamil Nadu 632014, India

2 School of Electronics Engineering, Vellore Institute of Technology, Vellore, Tamil Nadu, India

3 Rungta College of Engineering and Technology, Bhilai, India

and heat capacity [1]. Therefore, researchers have opted to study for multifunctional and lightweight materials to represent a conventional system with several parameters and so honeycomb composites came into the picture. Honeycomb sandwich composite structures have low density but they show high performance, stiffness and strength and so they are highly used in applications of marine and aerospace structures. Their geometry is designed in such a way that they possess high strength-to-weight and stiffness-to-weight ratios [2]. The strength of sandwich structures is determined by the size of the panel and the density of the cells. Using the statistical approach of sandwich composites made of honeycomb core deals how much load that the specimen can sustain by analyzing damages under different conditions. Sandwich panels shown in Fig. 1 are mainly comprised of two outer faces that are adhered to a thick core. Because they impart high rigidity to the structure, the outermost face sheets are comprised of stiffer and strong materials, often fiber-reinforced polymer. The core is typically light and has a low modulus of elasticity. Face sheet is typically a structural

Fig. 1 Schematic diagram of sandwich panel
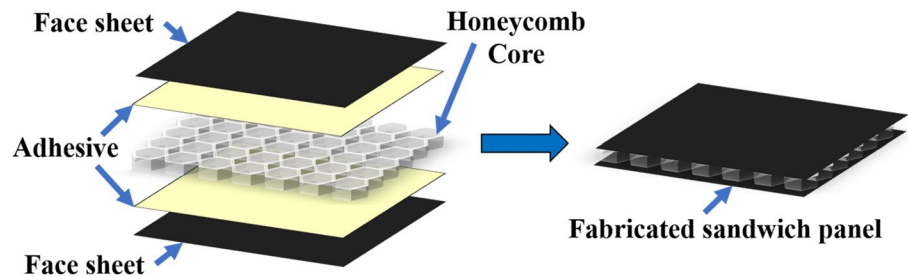
sandwich that contains the strongest material and thickness throughout and mainly resists in-plane and bending stresses.

Static behavior deals with the load-carrying ability of the structure and the failure modes present at each phase. For this, three-point bending test is carried out on the specimen. Lu et al. [3] examined the mechanical performance and stress distribution exposed to bending force. At load 7.2 kN, interfacial debonding is observed in the specimen. In three-point bending test, the honeycomb breaks down at 6.8 kN. Swagatika and Padhi [4] examined the compressive behavior of a honeycomb sandwich with face sheets of E-glass, basalt fiber and aluminum (Al) honeycomb core. The static and modal analysis of the composite beam was performed in ANSYS under static load conditions. The basalt fiber showed less deformation and equivalent stress. Anandan et al. [5] conducted experiments and simulations under the influence of increased temperatures. When the temperature was raised to 100 °C, the strength reduced by 9.2 percent while the stiffness remained constant. Babu et al. [6] evaluated the mechanical properties of CNT-reinforced fiber-reinforced plastic (FRP) honeycomb sandwich and performed tensile and compressive strength tests. They observed that the addition of CNT beyond 2% decreases the strength of the composite. Fan et al. [7] investigated on compression and bending performance of carbon-fiber-reinforced lattice core sandwich structure. Failures criteria were suggested and gave consistent analytical problems. Wei et al. [8] performed bending characteristics of all composite hexagon honeycomb sandwich beams through an experimental test and three-dimensional failure mechanism map. The insights provide the flexural property of the sandwich structure. Wu et al. [9] examined the static and fatigue behavior of Nomex honeycomb composite experimentally and the failure modes were analyzed using finite element analysis (FEA). The results of fatigue life were in good agreement and were similar to the experimental tests. Amulani et al. [2] investigated static and fatigue behavior on honeycomb sandwich using

different material combinations. Al-7075-T6 as honeycomb core and Ti–6Al–4 V as face sheet gave exceptional results. Shifa et al. [10] discussed the implications of adding carbon nanotubes on the hybrid honeycomb structure for high-tech applications. The results conclude that the compressive and flexural stiffness has been increased. Comparing to a flat sandwich panel, the inclusion of 0.2% multiwalled carbon nanotubes (MWCNT) enhanced performance by 21% and 28%, respectively.

In dynamic behavior, several vibration tests are carried out to analyze the modes, natural frequencies and some failure properties in the honeycomb structure. Yongqiang et al. [11, 12] investigated the vibration response of a honeycomb sandwich using various approaches. Selvaraj et al. [13] examined the vibration properties of multi-core sandwich beams. The experiment and simulation results of natural frequency were in good agreement. The effect of various core materials, thickness ratios and fiber angle orientations on the frequency response were investigated under various end situations. Redmann et al. [14] studied high-performance airframe construction with two honeycomb cores of Al and aramid. The damping of the sandwich panel was affected by static load and core material. Ragavan and Pitchipoo [15] examined the mechanical response of Al3003 honeycomb with 0.4 mm cell-wall thickness after being covered with carbon fiber epoxy composite layers. The results show that increasing the core thickness improved the damping behavior of the sandwich composites. Demircioglu et al. [16] studied free vibration tests of asymmetrical sandwich structures under clamped-free boundary conditions. As a consequence of the findings, it was determined that natural frequencies altered from symmetric to asymmetric arrangement. Praveen et al. [17] examined the forced and free vibration responses of a composite sandwich plate made of CNT-reinforced polymer. Furthermore, the transverse vibration responses of honeycomb sandwich structures are analyzed at various weight percent CNT, and results are compared to

those obtained without the presence of CNT. Ameri et al. [18] analyzed the effect of honeycomb core on free vibration analysis of fiber metal laminate beams compared to conventional composites. The layup pattern was made by hand-free technique and subjected to clamp-free boundary conditions. Natural frequencies and mode shapes were analyzed and compared.

Abbadi et al. [19] investigated the fatigue behavior of aramid mid-core and flaws experimentally and determined that the L configuration was more significant than the W configuration at the same load levels. Belan et al. [20] conducted fatigue tests on titanium Ti–6Al–4V alloy and concluded that three-point bending loads were more suitable than pull–push loads. Fatigue cracks were less common at lower amplitudes and more common at higher amplitudes. Shi et al. [21] performed flexural strength and energy absorption characteristics on honeycomb sandwich structures reinforced by aluminum grid. The results indicated that the ortho-grid aluminum with carbon fiber showed high structural properties for thin wall structures. Xiao et al. [22] studied dynamic impact test conditions along with the failures and energy absorption. Under axial impact, failure modes include lateral bending, lateral shear and local buckling. Large layup angles [90°]'s are particularly susceptible to lateral shear failure and have a high utilization rate. Kim and Cho [23] demonstrated the behavior of honeycomb sandwich composite structure with Al core after impact. They were subjected to different energies—50 J, 70 J and 100 J. At maximum load, the top face sheet breaks down. Maharjan et al. [24] discovered that laser shock peening (LSP) might modify the surface and improve fatigue performance. Severe plastic deformation at the surface occurred, resulting in microstructure refinement and residual stresses. Failure modes, shear and compression response were investigated by Lee et al. [25] when the temperature reaches 300 °C, the compressive and shear strengths fall. Four-point bending tests were used to assess toughness with regard to the loading rate.

Salam and Bondok [26] modeled the sandwich beams to compute the flexural stiffness and dynamic properties of sandwich beams. Sandwich beams with multilayer cores, multicells and holes in their cores of various forms and orientations were explored that indicate by increasing the number of cores or cells, the kinematic and dynamic response of the sandwich beams may be modified. Ozen et al. [27] studied the impact energy response of carbon fiber sandwich composite with thermoplastic as honeycomb re-entrant core experimentally and numerically. By the conclusion, in-plane re-entrant base core composite sandwich gives higher strength of impact and energies dissipation rate as compared to the in-plane and out-plane honeycomb core sandwich composite panel. Liu et al. [28] discovered that specific energy absorption (SEA) can extensively reflect crashworthiness and the Poisson ratio had a similar influence by creating parameters such as plateau stress, densified strain and relative density.

Several experiments were conducted including carbon-fiber-reinforced polymer (CFRP) as skin in the honeycomb composites. The reason behind the addition of CNT is to increase the strength of the composite structure with very little incorporation in weight [29, 30]. Saraswathy et al. [31] tested and observed vibration properties of sandwich structures with repeated debonding at the interface of the CFRP face sheet and honeycomb core. They showed that continuous debonding could lead to a larger drop in beam frequencies when compared to an intact beam. Yuan et al. [32] studied the effect of projectile mass on the damage behaviors of CFRP and discovered smaller dimension projectiles created localized and visible dent damage on the specimen with low energy impact, whereas bigger ones induced delamination for high energy impact. Audibert et al. [33] studied low-velocity impact tests on CFRP composite skin and Nomex as honeycomb core. The findings revealed that identifying skin damage and delamination using a basic compression and shear test. However, skin damage and delamination were not correctly predicted. Tang et al. [34] examined the damage of CFRP foam with Al sandwich structure with respect to the impact of high velocity and experimentally researched. He et al. [35] studied the low-velocity impact response and damage behavior of an Al-honeycomb sandwich structure with CFRP face sheets. They concluded the thickness of face sheet produced high influence on the impact resistance of honeycomb structures. Impact load of Al foam increases with increasing impact of velocities. Baba and Gibson [36] studied the effect vibration characteristics of sandwich composite CFRP with foam as core. They concluded that delamination affects the stiffness of the beam and results in changes of natural frequencies. Pechlivan et al. [37] investigated the compression behavior of CFRP honeycomb with various cell configurations. The thickness of the cell wall was the key element in the overall crushing reaction of CFRP honeycomb and it was unaffected by height. Liu et al. [38] examined quasi-static axial crushing, the failure mechanism and crashworthiness features with CFRP tubes and Al-honeycomb core. The cell width was paramount constraint affecting crashworthiness attributes.

Chowdhary et al. [39] performed vibration tests and compared results with and without MWCNT honeycomb sandwich. They concluded that natural frequency was higher when 1.5% MWCNT was used in all the types of composites and it was due to high stiffness in the face sheet. Caglayan et al. [40] used neat and CNT-reinforced PU foam-cored sandwich and performed three-point tests using different ASTM standards. CNT-reinforced composite was found to be stiffer and ASTM C393-16 gave acceptable failure modes. Ngoma et al. [41] have considered 2.5, 5, 7.5 and 10 wt% CNT volume fraction in their analysis. Shi et al. [42] showed that in the 7.5 percent concentration sample, a large amount of CNTs are concentrated in aggregates. The spatial distribution of CNTs in the matrix is nonuniform such that some local regions have a higher concentration of CNTs than the average volume fraction in the material. Hence in order to avoid agglomeration, in this study the volume fraction is restricted to 7.5 w%. Moreover, dispersion techniques/ time also significantly affected the CNTs morphology and resulting characteristics of the CNT-reinforced nanocomposites [43].

Recently Li et al. [44] proposed plate-reinforced dual functional micro lattice metamaterial (PDMMs) that shows elastic isotropy, dual crushing stages with a specific energy absorption up to 25.82 kj/kg and ultra-broadband sound absorption from 0.97 to 6.30 kHz. In another research article, Li et al. [45] also investigated the compressive responses of fractal-like honeycombs with different array configurations subjected to low-velocity impact loading environments. Further, Wang et al. [46] investigated the mechanical reinforcement mechanism of a hierarchical Kagome honeycomb structure.

Despite these, experimental and analytical work regarding the flexural test and free vibration test combined on the honeycomb sandwich with the specified combination is limited. At present, material failure is one of the important problems that the aerospace and marine industries are facing. In the present work, experimental work is carried out in which the four specimens were designed and undergone several tests. In specimen-I, Al3003 as core and carbon fiber with epoxy resins as face sheets have been fabricated as sandwich composite honeycomb structures and others namely specimen-II, specimen-III and specimen-IV, carbon fiber has been reinforced with epoxy including 2, 5 and 7.5 w% CNT as face sheets as a sandwich honeycomb composite structure.

The static response was performed and carried out under the three-point bending test using ASTM standard C393 and the same will be performed with the computational approach using ANSYS Workbench. The results achieved will be observed and compared for a better understanding of the static and dynamic approach of the composite structure. The static deformation along with maximum load and flexural stress were observed to understand the flexural strength. Further, to understand the dynamic behavior, free vibration test has been performed to achieve the mode shapes and corresponding natural frequencies for each specimen.

2 Materials and methods

2.1 Materials specification

In our proposed work, four specimens are designed and fabricated to form the sandwich structure. The honeycomb core designed is made up of Al3003 and used in all samples. In specimen-I, 4-ply unidirectional carbon fiber [0/90's] is fabricated on the core to form the sandwich structure. In specimen-II, epoxy and 2 w% CNT (carbon nanotubes) are added to carbon fiber. In specimen-III, epoxy and 5 w% CNT are reinforced with carbon fiber and in specimen-IV, 7.5 w% CNT is incorporated with carbon fiber. MWCNTs (lengths 1–5 μm and diameters 5–40 nm) have been used in the present investigation. The addition of CNT will offer good corrosion resistance, high weldability and high strength whereas carbon fiber as face sheets offers higher stiffness to resist higher forces due to loading and has a tendency to bear

**Table 2** Properties of core and face sheet

Properties	Al3003 core	Carbon-fiber-reinforced polymer (CFRP) face sheet
Density (g/cc)	0.08	1.60
Poisson's ratio	0.33	0.3
Modulus of elasticity (MPa)	1000	10,000
Bulk modulus (MPa)	980.4	8333.3
Tensile strength (MPa)	4.60	50
Shear modulus (MPa)	440	5000
Shear strength (MPa)	2.40	70

Table 1 Sandwich honeycomb composite combination

Samples	Core	Face sheet
Specimen-I	Al3003	4-ply UD carbon fiber, top and bottom face each
Specimen-II	Al3003	4-ply UD carbon fiber + 2 w% CNT, top and bottom face each
Specimen-III	Al3003	4-ply UD carbon fiber + 5 w% CNT, top and bottom face each
Specimen-IV	Al3003	4-ply UD carbon fiber + 7.5 w% CNT, top and bottom face each

Table 3 Dimensions of honeycomb sandwich composite

| Length L (mm)	Width b (mm)	Skin thickness t (mm)	Height of the core h (mm)	Length of cell edge l (mm)	Thickness of core wall d (mm)
150	25	1	10	6.35	0.06
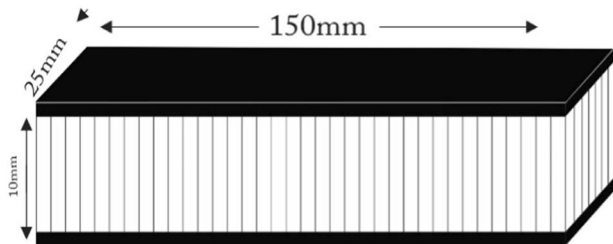
Fig. 2 Dimensions of honeycomb sandwich specimen

bending and tensile loads. Table 1 displays the combinations taken to form composite panels and Table 2 describes the mechanical properties of Al3003 and CFRP.

2.2 Geometry of honeycomb structure

During experimental tests, four honeycomb sandwich composites were designed with the combinations shown in Table 1. The dimensions of the honeycomb core are $150 \times 25 \times 10$ mm and the overall sandwich structure formed was $150 \times 25 \times 12$ mm. The thickness of face sheets was kept as 1 mm on top and bottom. Table 3 shows the specifications listed in detail (Fig. 2).

2.3 Fabrication of honeycomb sandwich composites

While preparing specimen-I, the mixture of epoxy LY556 and hardener HY951 was prepared with a weight ratio of 9:1 and the carbon fiber was cut into the face sheet dimensions.
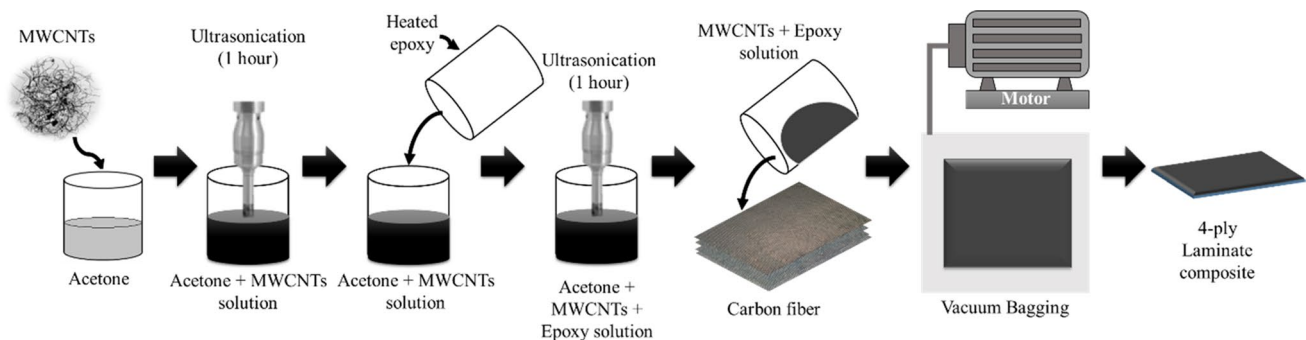
The mixture formed was applied on the carbon fiber in the direction of ply orientation by hand layup method. Next, vacuum bagging was done for 15 min at 20 bar pressure in order to remove excess resins and the specimen was kept for 24 h for curing. Finally, the core and face sheet of the specified given dimension were expurgated and pasted with araldite adhesives and the specimen will be fabricated. For other combinations, i.e., specimen-II, specimen-III and specimen-IV, sonication process was needed as shown in Fig. 3. The major difference between these combinations and the first specimen is the incorporation of CNT weight along with the carbon fiber and resins. Here, the weight of CNT as 2, 5 and 7.5 w% was taken. It requires a sonication process for an hour. Sonication was mainly performed to enhance the dispersibility, solubility and entanglement of CNTs. Meanwhile, epoxy was heated to reduce the viscosity and again sonication has been done with the heated epoxy and CNT–acetone solution for an hour. If acetone remains, the CNT–epoxy solution is heated at 70 °C for 15–20 min.

2.4 Static three-point bending test

Three-point bending tests or commonly known as flexure testing is a technique used for determining behavior of materials under static loads. It is highly used in flexible materials such as polymers, wood and composites. It was performed on the INSTRON-8801 by placing a specimen on two support anvils and applying continuous load at the center.

In this test, the area of uniform stress is quite small and concentrated under the mid-span loading. The three-point bending load configurations were done as per the ASTM standard C393. The investigation of flexural strength, displacement and damage modes of failure was carried out. Figure 4 depicts the experimental setup of the testing machine. For each specimen, the test was performed twice and the best results have been taken into account (Fig. 5).

Fig. 3 Schematic showing preparation procedure followed for fabrication of specimen-II, specimen-III and specimen-IV

Fig. 4 Photographic images of the specimens: **a** cutting face sheet and core and **b** final honeycomb sandwich
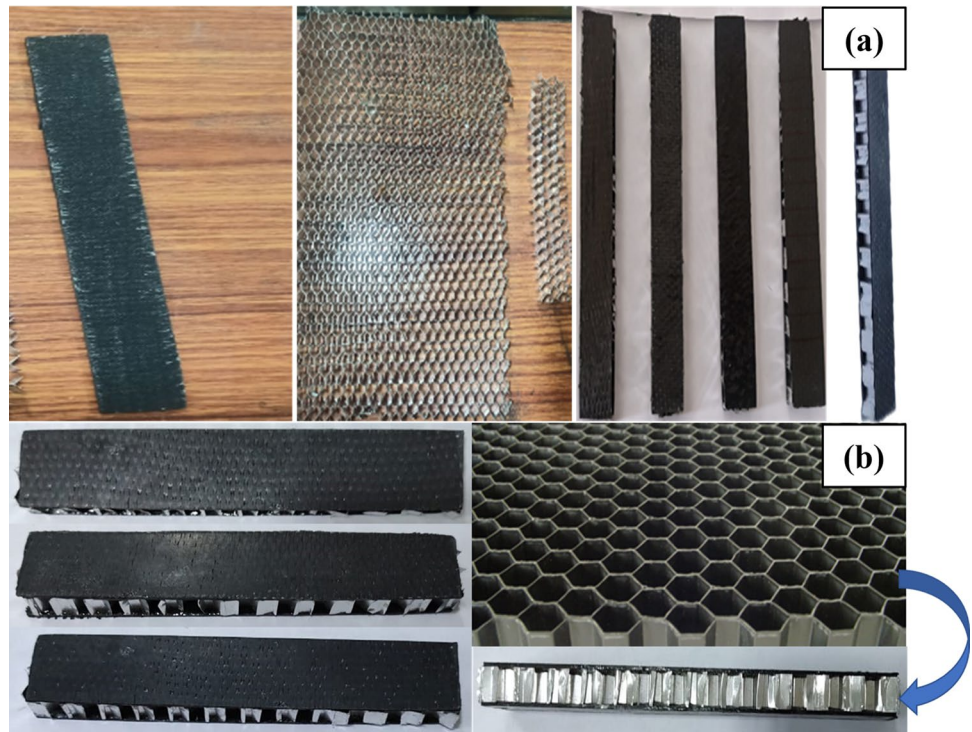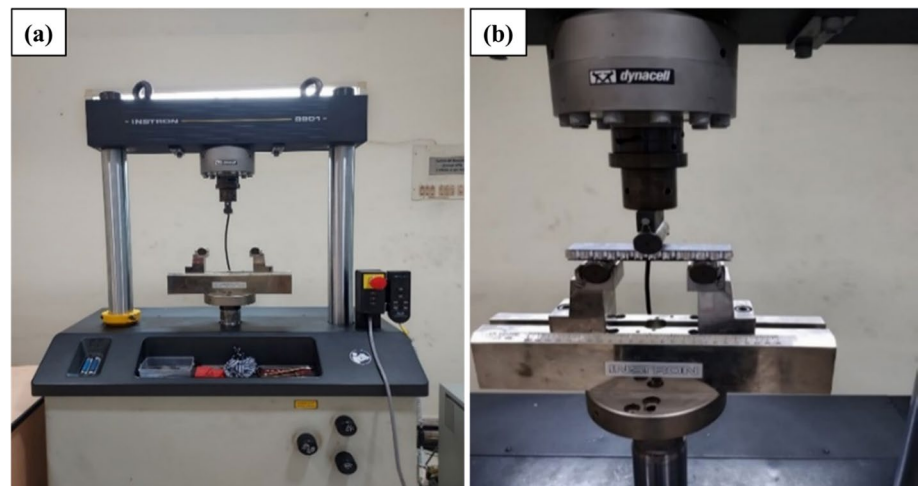

Fig. 5 Experimental setup of three-point flexural test: **a** INSTRON-8801 machine and **b** specimen placed with boundary conditions

2.5 Free vibration test

Free vibration test includes an impact hammer excitation approach as shown in Fig. 6. It is used to investigate the vibrational characteristics of manufactured sandwich composites. For natural frequencies, experiments were carried out on constructed carbon fiber and carbon fiber/CNT sandwich specimens under cantilever boundary conditions. The specimens were initially mounted on the steel fixture. The data acquisition system (DAQ Model No. NI9234) was then connected to the computer, with the other end of the DAQ attached to the impulse hammer and accelerometer.

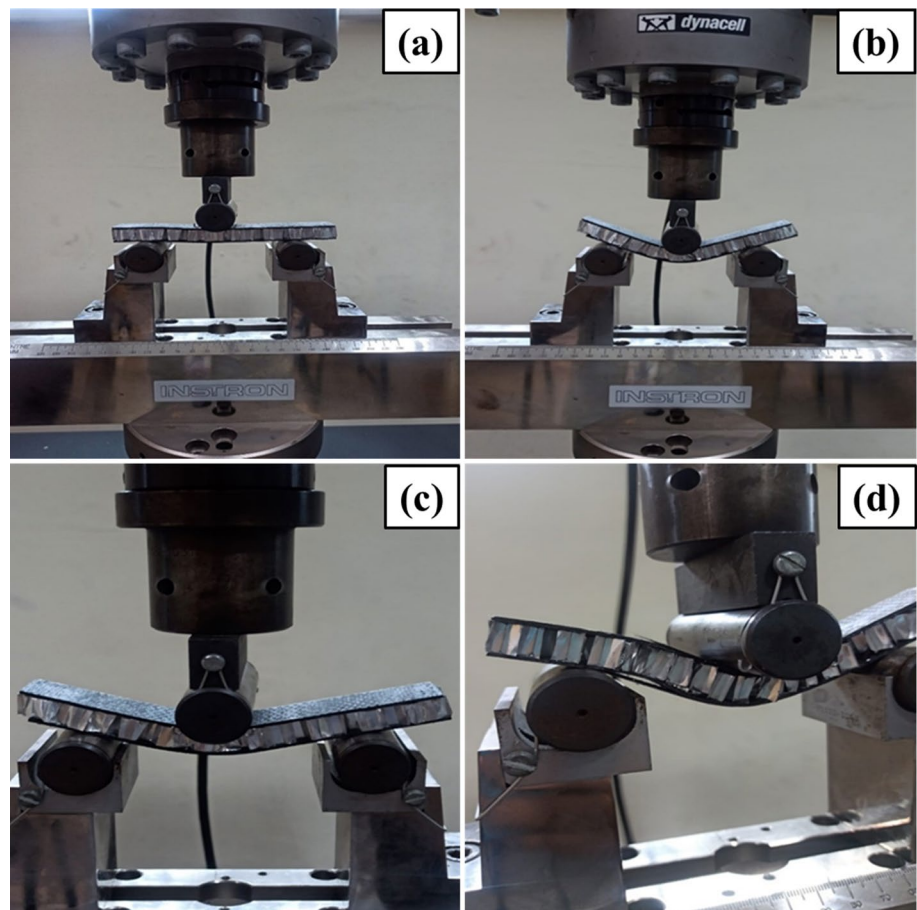**Fig. 6** Free vibration test experimental setup
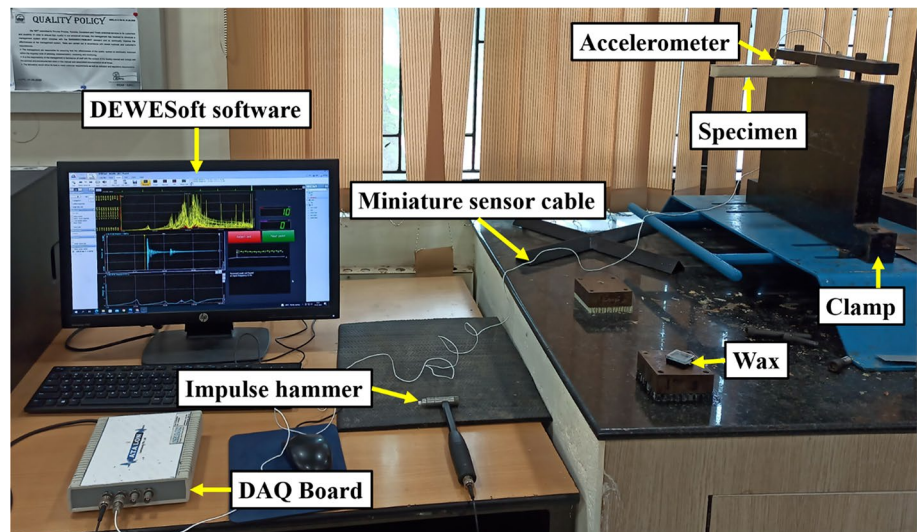
Fig. 7 Phases under three-point bending test: **a** applied load, **b** inter-laminar shear failure and bending of cell wall, **c** compression and face yielding and **d** core crushing

The shear sensor (Model No. 352C22) was put on the top surface of the specimen to capture acceleration data and the impulse hammer (Model No. 5800SL) was used to stimulate all nodal locations of the cantilevered sandwich beam. The DAQ system was utilized to convert acceleration response data to frequency response function at all eleven nodes of the sandwich beam, which can be observed on the display unit via DEWESOFT software.

Measurements were taken for multiple trials in order to achieve reproducibility of results. The blasting and impact procedures are used in the majority of documented examples on the dynamic characteristics of sandwich constructions.

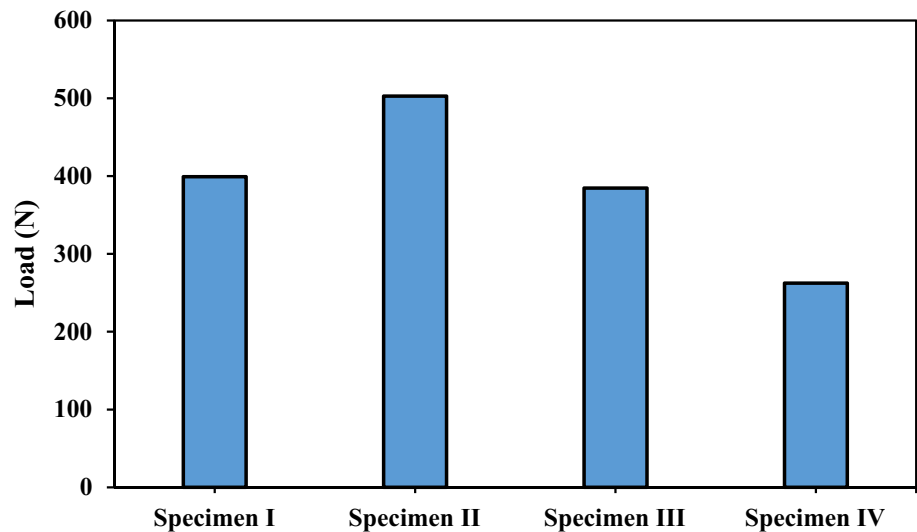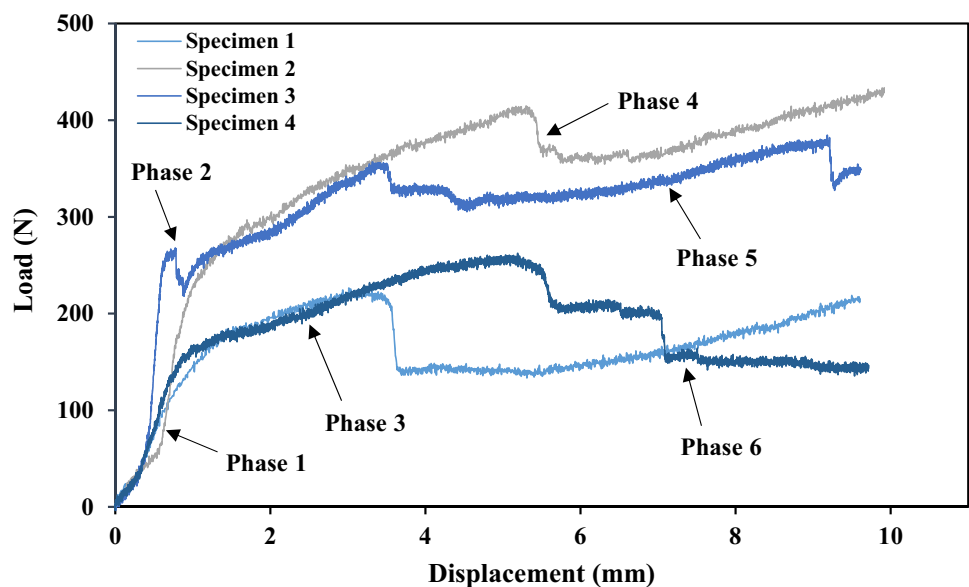**Fig. 8** Maximum load-carrying ability for specimens

Fig. 9 Flexural load variation with displacement for specimens

## 3 Results and discussion

3.1 Static three-point bending test

The experimental investigation of the flexural strength was performed as shown in Fig. 7. The load was applied at the mid of the span and deflection was recorded till the specimen fails. Figure 8 displays the maximum load value for each specimen after the experiments were done. At continuous loads, the displacement was noted and damage modes were observed in different phases as shown in Fig. 9. Face yielding and compression on the face sheet were witnessed. It was mainly due to the stresses and the elastic nature of the material. On further loading, the composite bends until cracks are observed in the face sheet and the specimen finally breaks down.

Figure 9 describes the variation between load and displacement of all four specimens. In the first phase, a linear

Fig. 10 Variation between flexural stress and strain for specimens
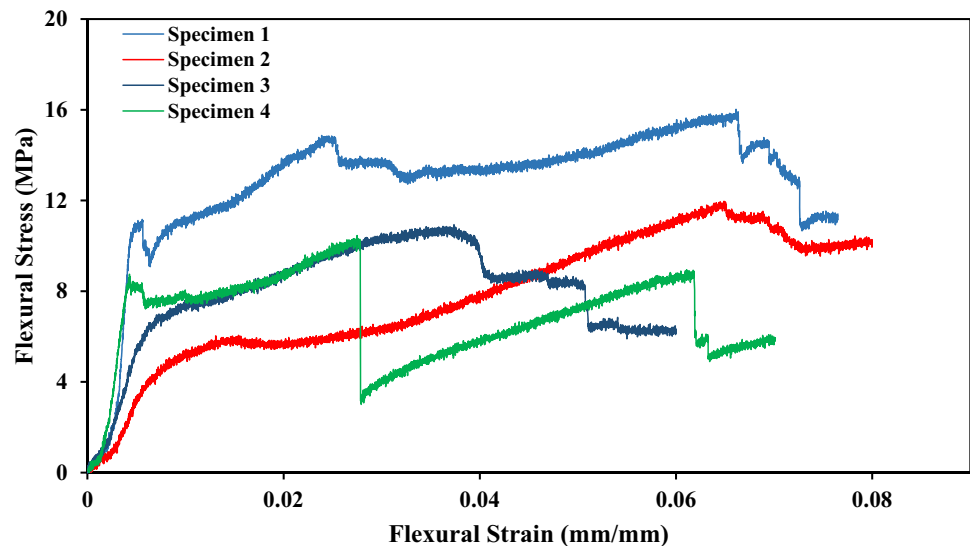
relationship was observed between load and displacement. With an increase in load, the displacement moves with a small value and it concludes yielding of face sheet as depicted in phase 2. Moreover, the small peak load was observed at this phase. But with a further increase in force, a sudden decrease in load-carrying capability was seen in the specimen. With further displacement, the highest peak was attained for specimens III and IV at phase 3. This indicates the highest load-bearing capacity of the specimen. Further, displacement was observed with the sudden drop in load at phase 4. Phase 5 indicates an increase in displacement with the application of further loads. Although, specimens I and II witnessed the highest load values in this phase. In phase 6, the load was nearly constant and displacement kept on increasing until the specimen failed completely. It was observed that with the addition of CNT in carbon fiber, the strength of the material increases. But beyond adding 2 w% CNT, the strength starts decreasing due to the effect of agglomeration [5].

Figure 10 shows the variation of maximum stress with an increase in strain for all the specimens. We obtained that maximum load specimen-I can withstand was 399.21 N and the maximum bending stress corresponding to it was 16.633 MPa. The flexural stress at yield (zero slope) was found to be 9.438 MPa and flexural strain corresponding to it was 0.13202 mm/mm. It shows that the specimen has the tendency of load carrying and the material will fail at higher value. The maximum load for specimen-II was recorded as 502.76 N and the maximum bending stress was 20.94830 MPa. The flexural stress at yield (zero slope)

was obtained as 17.27367 MPa and flexural strain at was 0.10674 mm/mm. For specimen-III, the maximum load achieved was 384.51 N and maximum flexural stress was 16.021 MPa. The flexural strain at maximum flexural stress is 0.06611 mm/mm. In specimen-IV, the maximum load value was found to be 262.38 N and maximum flexural stress to be 10.9324 MPa. The flexural strain was obtained as 0.03786 mm/mm. Due to agglomeration, load-carrying capacity was decreased by adding beyond 2 w% CNT to carbon fiber face sheet. In the concentration regime at which nanoparticle aggregation is expected, the strain at yield was observed to decrease continuously with addition of CNTs but the stress increased in 2 w% CNT addition and then started decreasing at yield. It is evident from the results that addition of CNT significantly improves the strength of the composite. On the other hand, agglomeration of CNT decreases the property slightly but still provides the results better than the conventional composites.

3.2 Failure modes in honeycomb composite

The failure modes were observed during the bending test and they are mentioned in Fig. 11. Figure 7 shows that during the bending test, compression and yielding on face sheet were noticed. The reason was mainly due to the stresses acting along the face sheet exceeding elastic limit of the material. Further load on the specimen resulted in inter-laminar shear failure and bending of the cell wall as shown in Fig. 11. The reason behind failure was wrinkling whereas the core failed due to shearing and crushing of material when the

Fig. 11 Failures modes of honeycomb sandwich composite: **a** delamination, **b** debonding, **c** inter-laminar shear failure, **d** crushing and **e** face sheet failure
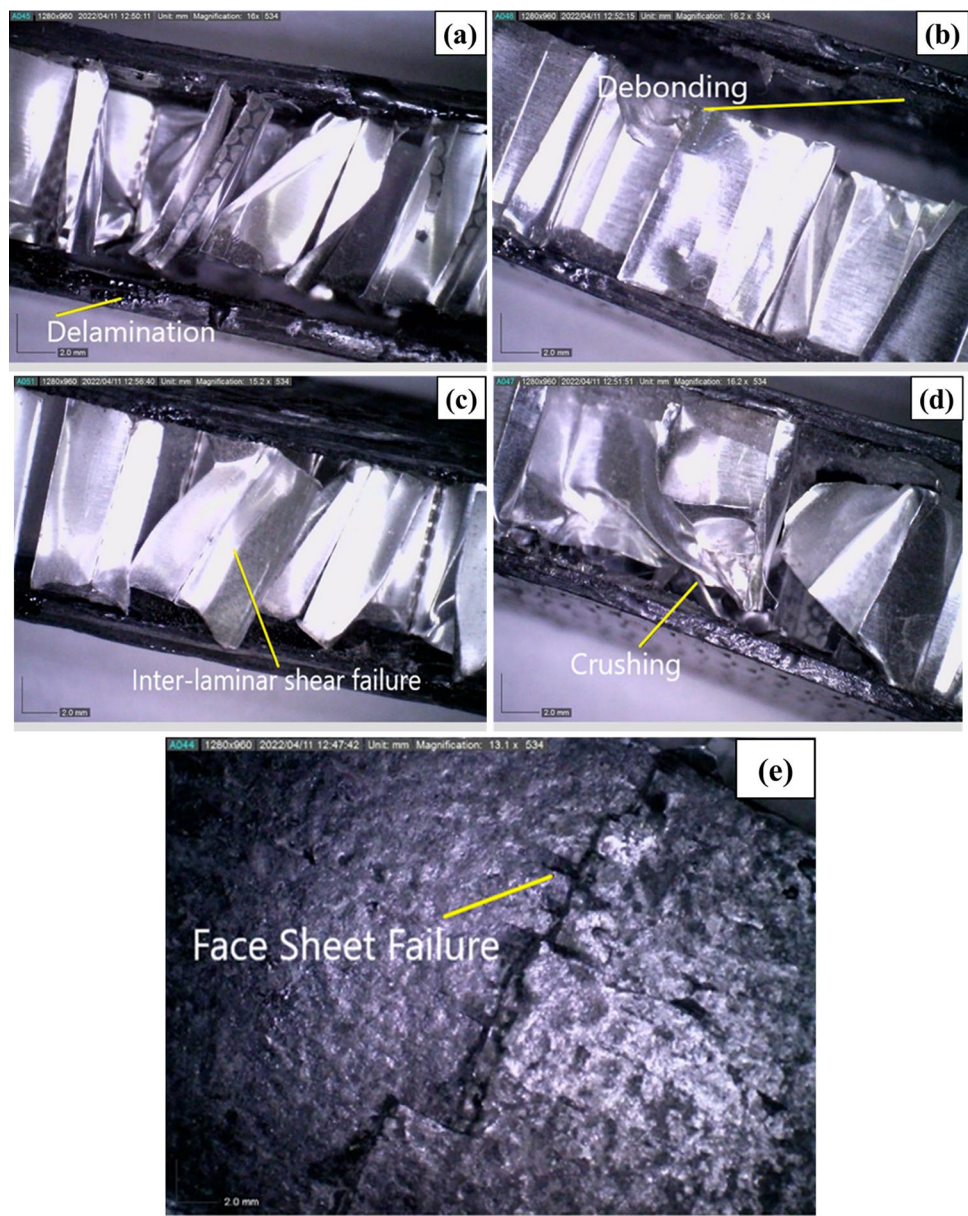
shear stress of the core reached the shear strength during the time of bending. When the load was applied at beginning, core crushing was witnessed first for very short span of time because short columns experienced heavy loads. With increase in displacement, delamination occurs and the layers of plies get damaged later resulting in debonding and the face sheet gets detached from the core. Further with the application of load, inter shear laminar failure was seen which was due to bending of cell wall. The crushing of the core was observed as the cell wall doesn't have enough strength to withstand the load. Finally, the face sheet breaks and the composite is broken completely.

3.3 Computational validation of bending test

The finite numerical model was established for specimen-I, a method to solve engineering problems to the nearest approximations. The honeycomb specimen was designed in
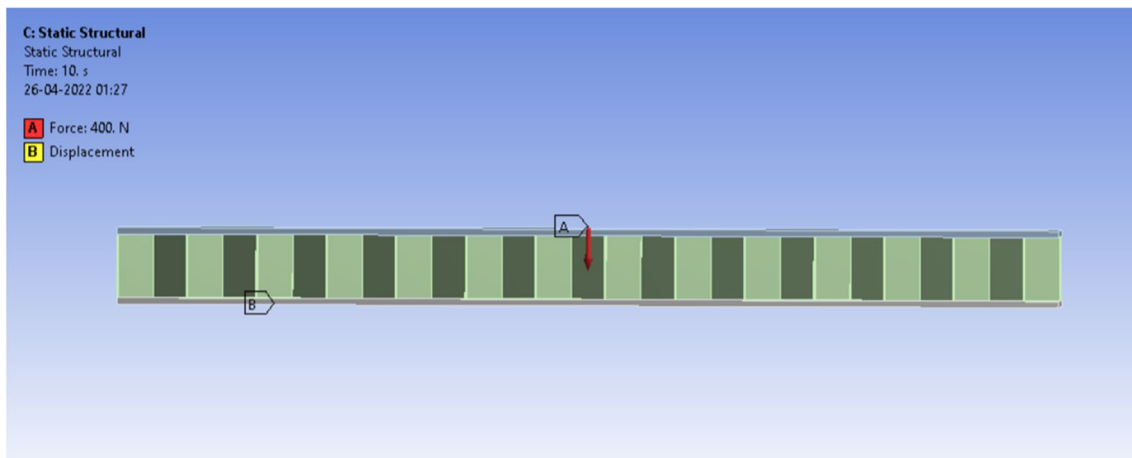
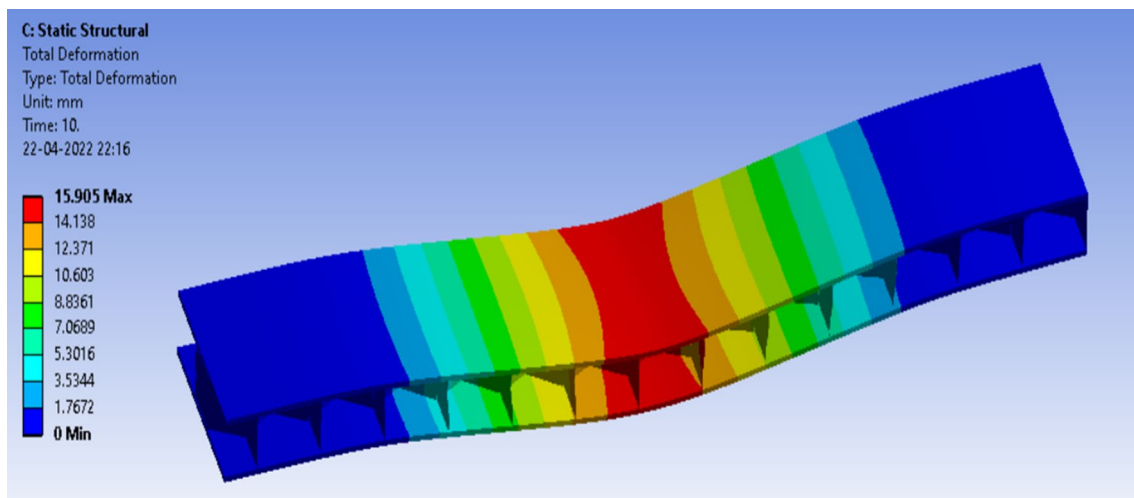**Fig. 12** Boundary conditions at maximum load

Fig. 13 Deformation at maximum load for specimen-I

Solidworks and later imported into ANSYS Workbench. The material properties of Al3003 and carbon fiber were added to the engineering library. In the design modeler, three-point bending setup was done taking ASTM standard C393 into consideration. In static structural, the materials were selected for core and face sheet. The contact and target bodies were solid. To obtain a refined mesh with the best possible results, patch conforming algorithm was taken under consideration under tetrahedron method. The body sizing and face sizing was selected to 2 mm. Figure 12 shows the

Fig. 14 Variation of load with deformation for specimen-I
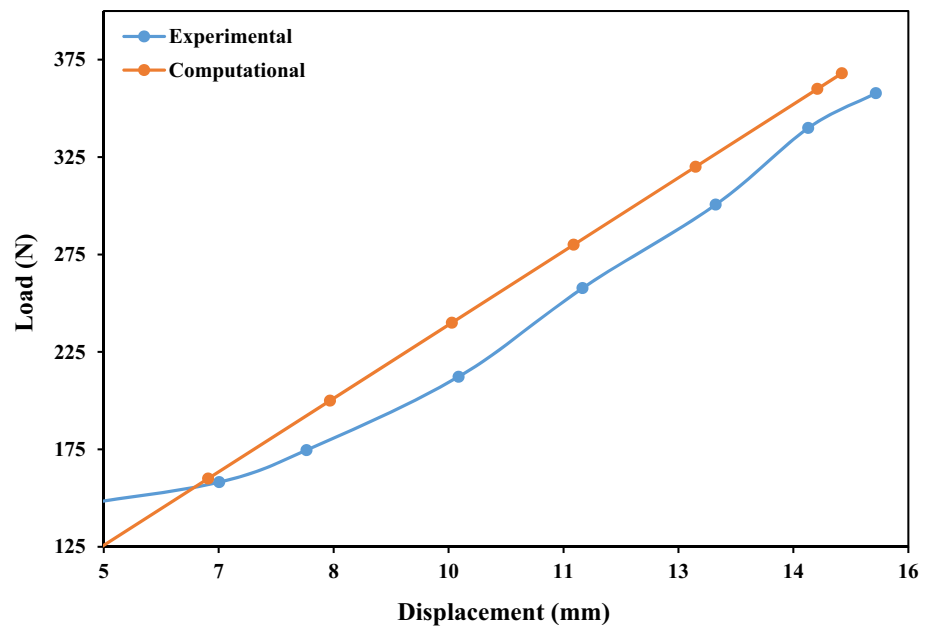
Table 4 Natural frequencies with three mode shapes for different combinations

Specimen	Natural frequencies (Hz)		
	Mode I	Mode II	Mode III
Specimen-I	336.98	802.03	1061.8
Specimen-II	325	831.25	1049.8
Specimen-III	385.02	855.48	1130.5
Specimen-IV	452.33	779.81	1915.3

boundary conditions on specimen-I. The load was applied at the mid-region of the specimen and the displacement representing the boundary was applied at both the ends of the span length.

The load values were selected from the experimental data and deformation corresponding to these values was obtained. Figure 13 shows the deformation which came around 15.905 mm at the maximum load 400 N. As the load was undistrubuted over the panel, it was confirmed that the maximum deformation will be observed at the central region and the lowest at the boundary areas [1]. The values of deformation were noted at various load values and comparison of results was achieved which can be witnessed in Fig. 14. It was observed that the displacement values of experimental and simulation results were similar.

3.4 Free vibration test

Free vibration characteristics of fabricated CFRP/Al3003 honeycomb sandwich composite were studied using the impact hammer excitation method. Mode shapes and natural frequencies were investigated for all specimens. For each specimen, three modal natural frequencies were extracted and are listed in Table 4. Figure 15 shows the results of specimen-I for mode shape-I. The combined response graph will be the same for all modes but single response graph varies with mode shapes. Looking at the mode shapes pattern in free vibration, the corresponding natural frequencies were observed for each mode shape. Figure 15c automatically generated from the software gives the value of damping factor.

Figures 16 and 17 depict mode shape-II and shape-III for specimen-I. The combined peal response graph for 11 nodes was nearly equal for all three mode shapes but the amplitude–frequency waveform and single response peak vary with respect to mode shape pattern. Therefore, we can conclude that mode shape patterns fluctuate with the individual response. The overall frequency response for specimen-I is shown in Fig. 18. Similarly, the vibration analysis of other specimens was noted. Figure 19 depicts the natural frequencies for all specimens taking three mode shapes, respectively. It was observed that the natural frequency increases with an increase in the mode shape. It also concludes that the sandwich
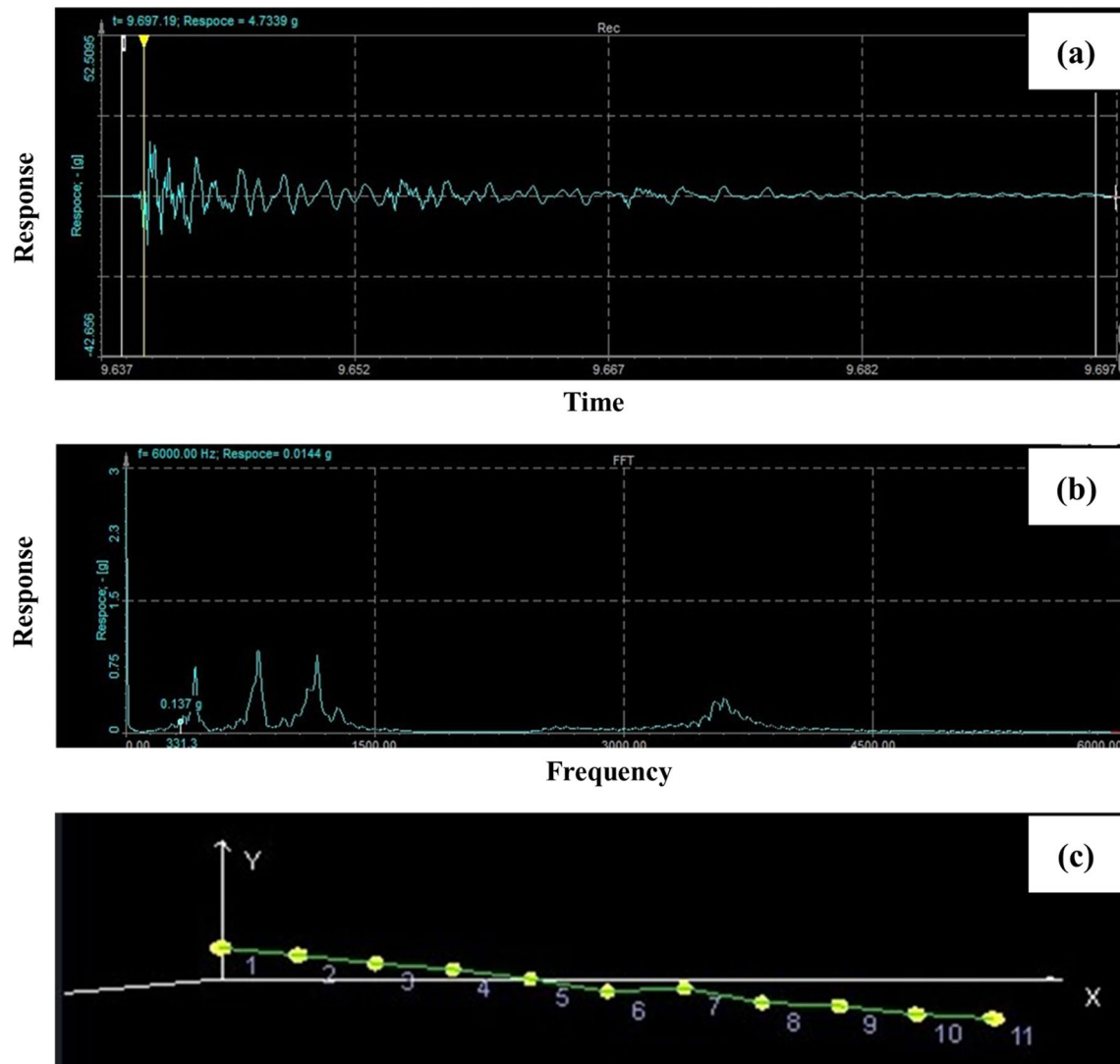
Fig. 15 Mode shape-I for specimen-I: **a** single response vs time, **b** amplitude–frequency waveform and **c** mode shape-I pattern

composite made by incorporating CNT shows high level of increment in the natural frequencies and the material is stiff. Finally, it can be observed from the results that due to addition of CNTs stiffness of the structure increased significantly which results in higher frequency.

4 Conclusions

In this investigation, static and dynamic behaviors for Al3003/CFRP honeycomb sandwich composites were investigated under three-point bending and free vibration test. Four different specimens were fabricated and the experiments were carried out. It was observed that honeycomb composites reinforced with 2 w% CNT increase the strength of the structure and beyond 2 w% CNT, the load-carrying ability decreases due to agglomeration. To avoid agglomeration and clustering, sonication dispersion approach has been used for achieving uniform dispersal of CNTs in carbon fiber–epoxy composites. Under three-point bend test, fabricated structure showed capability to withstand higher loads. The maximum load observed was 502.76 N and flexural stress was 20.94 MPa for specimen-II. Load and displacement results were also achieved
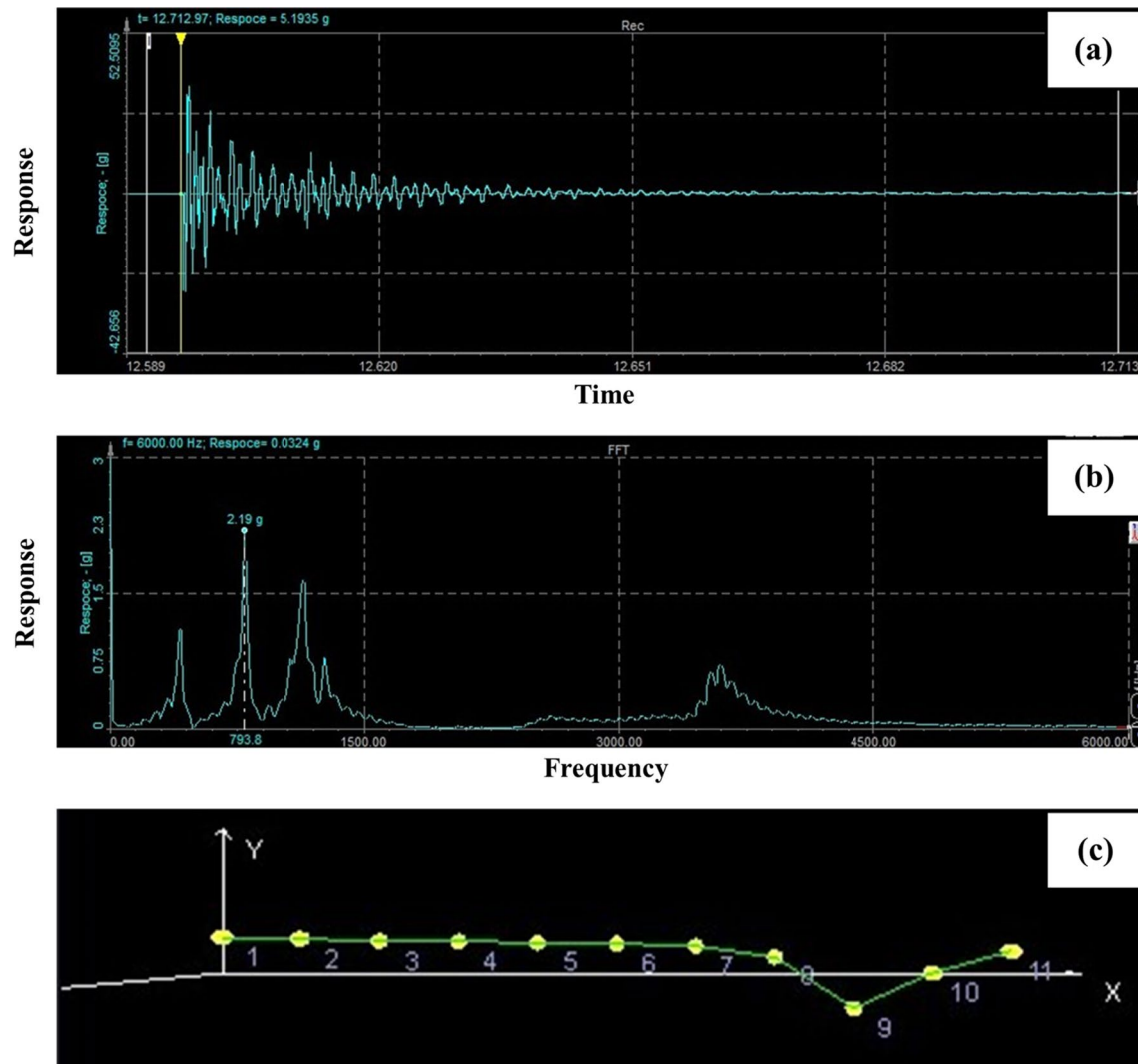
Fig. 16 Mode shape-II for specimen-I: **a** single response vs time, **b** amplitude–frequency waveform and **c** mode shape-II pattern

computationally and the comparison graph was plotted. The values were similar with the experimental data. For dynamic behavior, free vibration test was performed to analyze the natural frequency and mode shapes by using impact hammer excitation method. It was observed that the natural frequency increases with rise in mode shapes for all specimens. Each mode has its own natural frequency for the structure. The specimen reinforced with CNTs was found to be stiffer hence it reveals that as natural frequencies are dependent on material stiffness. The highest natural frequency was witnessed as 1915.3 Hz for specimen-IV. It is evident from the results that addition of CNT significantly improves the strength and stiffness of the composite. On the other hand agglomeration of CNT decreases the property slightly but still provides the results better than the conventional composites. Hence, addition of CNTs enhances the desired property of the proposed composite structures. The proposed study helps to investigate the material combination and parameters using statistical and dynamical approaches in a way to achieve better structure characteristics that have aerospace, automobile and marine applications.
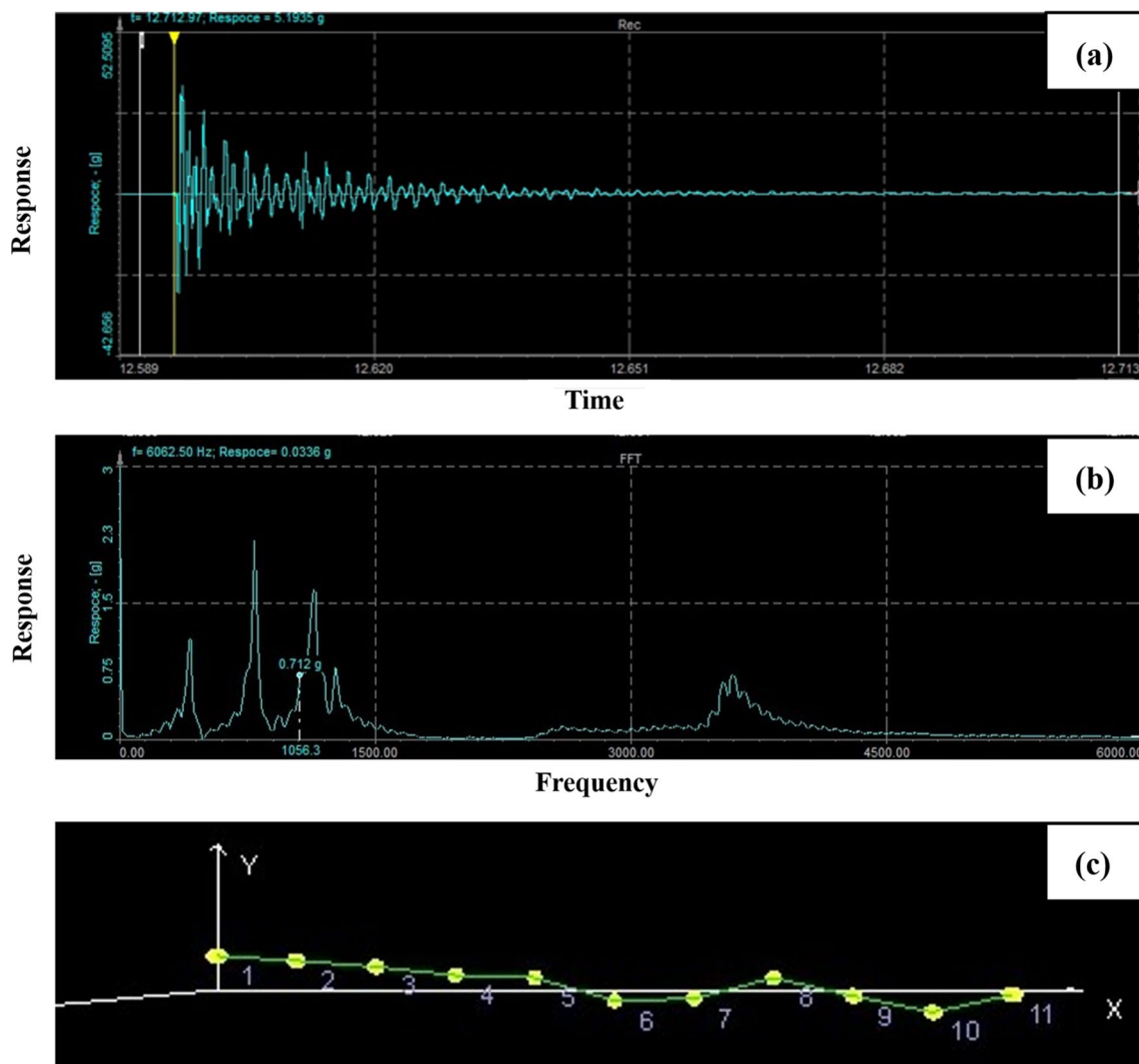
Fig. 17 Mode shape-III for specimen-I: **a** single response vs time, **b** amplitude–frequency waveform and **c** mode shape-III pattern
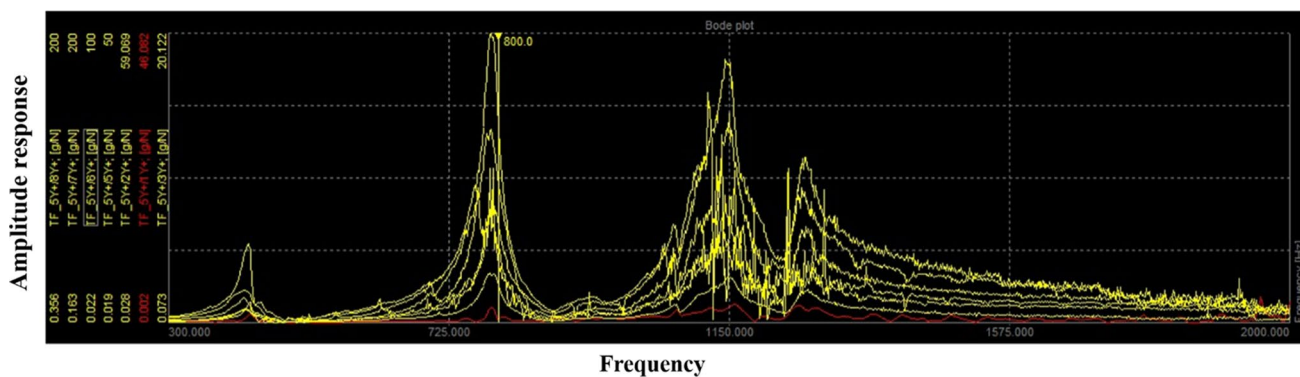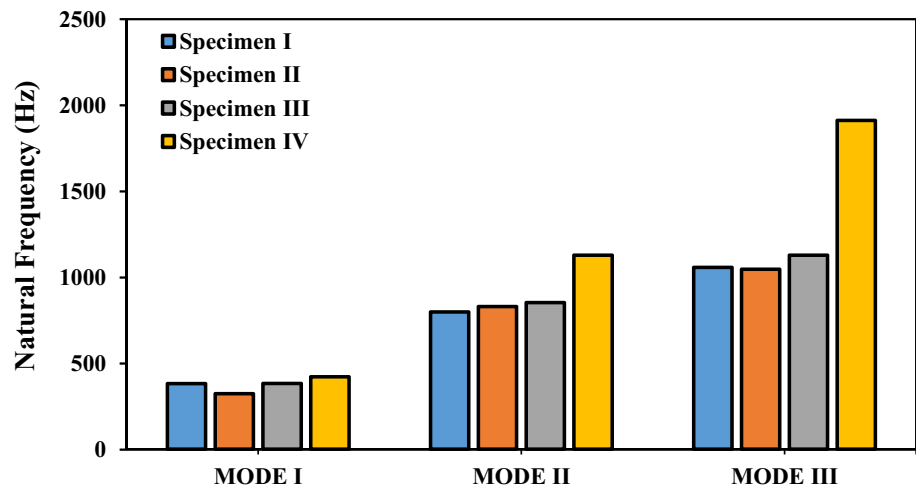

Fig. 18 Combined amplitude–frequency response graph of specimen-I for all nodes

Fig. 19 Natural frequencies obtained at mode shapes for specimens

References

1. Soni SK, Thomas B, Swain A, Roy T (2022) Functionally graded carbon nanotubes reinforced composite structures: an extensive review. Compos Struct 299:116075. https://doi.org/10.1016/j.compstruct.2022.116075
2. Amulani A, Pratap H, Thomas B (2021) Investigation of static and fatigue behavior of honeycomb sandwich structure: a computational approach. J Braz Soc Mech Sci Eng 43:476. https://doi.org/10.1007/s40430-021-03195-y
3. Lu C, Zhao M, Jie L et al (2015) Stress distribution on composite honeycomb sandwich structure suffered from bending load. Procedia Eng 99:405–412. https://doi.org/10.1016/j.proeng.2014.12.554
4. Swagatika S, Padhi A (2018) Static and dynamic analysis of basalt fiber reinforced sandwich composite laminates with aluminium honeycomb core. Int J Sci Res 7:622–630
5. Anandan S, Dhaliwal G, Ganguly S, Chandrashekhara K (2020) Investigation of sandwich composite failure under three-point bending: Simulation and experimental validation. J Sandw Struct Mater 22:1838–1858. https://doi.org/10.1177/1099636218791162
6. Suresh Babu KS, Bylappa BK, Shivanand HK (2017) Evaluation of mechanical properties of CNT reinforced FRP honeycomb core sandwich composites. Asian J Sci Technol 8:5311–5314
7. Fan H, Yang L, Sun F, Fang D (2013) Compression and bending performances of carbon fiber reinforced lattice-core sandwich composites. Compos Part A Appl Sci Manuf 52:118–125. https://doi.org/10.1016/j.compositesa.2013.04.013
8. Wei X, Wu Q, Gao Y, Xiong J (2020) Bending characteristics of all-composite hexagon honeycomb sandwich beams: experimental tests and a three-dimensional failure mechanism map. Mech Mater 148:103401. https://doi.org/10.1016/j.mechmat.2020.103401
9. Wu X, Yu H, Guo L et al (2019) Experimental and numerical investigation of static and fatigue behaviors of composites honeycomb sandwich structure. Compos Struct 213:165–172. https://doi.org/10.1016/j.compstruct.2019.01.081
10. Shifa M, Tariq F, Baloch RA (2017) Effect of Carbon nanotubes on mechanical properties of honeycomb. Nucleus 54
11. Yongqiang L, Dawei Z (2009) Free flexural vibration analysis of symmetric rectangular honeycomb panels using the improved Reddy's third-order plate theory. Compos Struct 88:33–39. https://doi.org/10.1016/j.compstruct.2008.03.033
12. Yongqiang L, Zhu Dawei LF (2010) Geometrically nonlinear free vibrations of the symmetric rectangular honeycomb sandwich panels with simply supported boundaries. Compos Struct 92:1110–1119. https://doi.org/10.1016/j.compstruct.2009.10.012
13. Selvaraj R, Gupta K, Singh SK et al (2021) Free vibration characteristics of multi-core sandwich composite beams: experimental and numerical investigation. Polym Polym Compos 29:S1414–S1423. https://doi.org/10.1177/09673911211057679
14. Redmann A, Montoya-Ospina MC, Karl R et al (2021) High-force dynamic mechanical analysis of composite sandwich panels for aerospace structures. Compos Part C Open Access 5:100136. https://doi.org/10.1016/j.jcomc.2021.100136
15. Ragavan R, Pitchipoo P (2020) Evaluation and modeling the static and free vibrational behaviours of AA3003/CFRP honeycomb sandwich structures. Mater Res Express 7:105604. https://doi.org/10.1088/2053-1591/abbfc0
16. Demircioğlu U, Yildiz AS, Çakir MT (2021) An investigation of the effect of asymmetry on the free vibration behavior of sandwich structure. Sakarya Univ J Sci. https://doi.org/10.16984/saufenbilder.955314
17. Praveen AP, Rajamohan V, Arumugam AB, Mathew AT (2020) Vibration analysis of a multifunctional hybrid composite honeycomb sandwich plate. J Sandw Struct Mater 22:2818–2860. https://doi.org/10.1177/1099636218820764
18. Ameri B, Moradi M, Talebitooti R (2021) Effect of honeycomb core on free vibration analysis of fiber metal laminate (FML) beams compared to conventional composites. Compos Struct 261:113281. https://doi.org/10.1016/j.compstruct.2020.113281
19. Abbadi A, Tixier C, Gilgert J, Azari Z (2015) Experimental study on the fatigue behaviour of honeycomb sandwich panels with artificial defects. Compos Struct 120:394–405. https://doi.org/10.1016/j.compstruct.2014.10.020
20. Belan J, Kuchariková L, Tillová E, Chalupová M (2019) Three-point bending fatigue test of TiAl6V4 titanium alloy at room temperature. Adv Mater Sci Eng 2019:1–11. https://doi.org/10.1155/2019/2842416
21. Shi S, Sun Z, Hu X, Chen H (2014) Flexural strength and energy absorption of carbon-fiber–aluminum-honeycomb composite sandwich reinforced by aluminum grid. Thin-Walled Struct 84:416–422. https://doi.org/10.1016/j.tws.2014.07.015
22. Xiao Y, Wen X, Liang D (2021) Failure modes and energy absorption mechanism of CFRP Thin-walled square beams filled with aluminum honeycomb under dynamic impact. Compos

Struct 271:114159. https://doi.org/10.1016/j.compstruct.2021.114159

23. Kim YC, Cho JU (2014) Comparative Study between impact behaviors of composites with aluminum foam and honeycomb. Curr Nanosci 10:23–27. https://doi.org/10.2174/1573413709999131205152839

24. Maharjan N, Chan SY, Ramesh T et al (2021) Fatigue performance of laser shock peened Ti6Al4V and Al6061-T6 alloys. Fatigue Fract Eng Mater Struct 44:733–747. https://doi.org/10.1111/ffe.13390

25. Lee HS, Hong SH, Lee JR, Kim YK (2002) Mechanical behavior and failure process during compressive and shear deformation of honeycomb composite at elevated temperatures. J Mater Sci 37:1265–1272. https://doi.org/10.1023/A:1014344228141

26. Abdel Salam M, Bondok NE (2010) Free vibration characteristics for different configurations of sandwich beams. Int J Mech Mechatron Eng 10:27–36

27. Özen İ, Çava K, Gedikli H et al (2020) Low-energy impact response of composite sandwich panels with thermoplastic honeycomb and reentrant cores. Thin-Walled Struct 156:106989. https://doi.org/10.1016/j.tws.2020.106989

28. Liu J, Chen W, Hao H, Wang Z (2021) In-plane crushing behaviors of hexagonal honeycombs with different Poisson's ratio induced by topological diversity. Thin-Walled Struct 159:107223. https://doi.org/10.1016/j.tws.2020.107223

29. Soni SK, Thomas B, Kar VR (2020) A comprehensive review on CNTs and CNT-reinforced composites: syntheses, characteristics and applications. Mater Today Commun 25:101546. https://doi.org/10.1016/j.mtcomm.2020.101546

30. Soni SK, Thomas B (2019) Influence of TiO2 and MWCNT nanoparticles dispersion on microstructure and mechanical properties of Al6061 matrix hybrid nanocomposites. Mater Res Express. https://doi.org/10.1088/2053-1591/ab5dfe

31. Saraswathy B, Mangal L, Kumar RR (2012) Analytical approach for modal characteristics of honeycomb sandwich beams with multiple debond. J Sandw Struct Mater 14:35–54. https://doi.org/10.1177/1099636211428804

32. Yuan K, Liu K, Wang Z et al (2021) Dynamic fracture in CFRP laminates: effect of projectile mass and dimension. Eng Fract Mech 251:107764. https://doi.org/10.1016/j.engfracmech.2021.107764

33. Audibert C, Andréani A-S, Lainé É, Grandidier J-C (2019) Discrete modelling of low-velocity impact on Nomex® honeycomb sandwich structures with CFRP skins. Compos Struct 207:108–118. https://doi.org/10.1016/j.compstruct.2018.09.047

34. Tang E, Zhang X, Han Y (2019) Experimental research on damage characteristics of CFRP/aluminum foam sandwich structure subjected to high velocity impact. J Market Res 8:4620–4630. https://doi.org/10.1016/j.jmrt.2019.08.006

35. He W, Yao L, Meng X et al (2019) Effect of structural parameters on low-velocity impact behavior of aluminum honeycomb sandwich structures with CFRP face sheets. Thin-Walled Struct 137:411–432. https://doi.org/10.1016/j.tws.2019.01.022

36. Baba BO, Gibson RF (2007) The vibration response of composite sandwich beam with delamination. Adv Compos Lett. https://doi.org/10.1177/096369350701600204

37. Pehlivan L, Baykasoğlu C (2019) An experimental study on the compressive response of CFRP honeycombs with various cell configurations. Compos B Eng 162:653–661. https://doi.org/10.1016/j.compositesb.2019.01.044

38. Liu Q, Mo Z, Wu Y et al (2016) Crush response of CFRP square tube filled with aluminum honeycomb. Compos B Eng 98:406–414. https://doi.org/10.1016/j.compositesb.2016.05.048

39. Chowdhary S, Tafesse B, Ananda Babu A, Muthukumaran G (2021) Prediction of influences of MWCNT fillers on the vibration characteristics of laminated hybrid honeycomb core sandwich GFRP composite plate. Mater Today Proc 47:6670–6675. https://doi.org/10.1016/j.matpr.2021.05.110

40. Caglayan C, Gurkan I, Gungor S, Cebeci H (2018) The effect of CNT-reinforced polyurethane foam cores to flexural properties of sandwich composites. Compos Part A Appl Sci Manuf 115:187–195. https://doi.org/10.1016/j.compositesa.2018.09.019

41. Ngoma MM, Mathaba M, Moothi K (2021) Effect of carbon nanotubes loading and pressure on the performance of a polyethersulfone (PES)/carbon nanotubes (CNT) membrane. Sci Rep 11:23805. https://doi.org/10.1038/s41598-021-03042-z

42. Shi D-L, Feng X-Q, Huang YY et al (2004) The effect of nanotube waviness and agglomeration on the elastic property of carbon nanotube-reinforced composites. J Eng Mater Technol 126:250–257. https://doi.org/10.1115/1.1751182

43. Soni SK, Tody V, Thomas B (2021) Influence of dispersion technique/time on dispersion stability, aspect ratio and morphology of multi-walled carbon nanotubes. Int J Nanotechnol 18:590. https://doi.org/10.1504/IJNT.2021.116176

44. Li Z, Shen L, Wei K, Wang Z (2021) Compressive behaviors of fractal-like honeycombs with different array configurations under low velocity impact loading. Thin-Walled Struct 163:107759. https://doi.org/10.1016/j.tws.2021.107759

45. Wang Z, Lei Z, Li Z et al (2021) Mechanical reinforcement mechanism of a hierarchical Kagome honeycomb. Thin-Walled Struct 167:108235. https://doi.org/10.1016/j.tws.2021.108235

46. Li Z, Zhai W, Li X et al (2022) Additively manufactured dual-functional metamaterials with customisable mechanical and sound-absorbing properties. Virtual Phys Prototyp 17:864–880. https://doi.org/10.1080/17452759.2022.2085119